Ambient Testing and Model Updating of a Bridge for High-Speed Trains

Reto Cantieni, rci dynamics, Structural Dynamics Consultants
Raubbuehlstrasse 21B, CH-8600 Duebendorf, Switzerland

Maik Brehm, Bauhaus Universität

Volkmar Zabel, Bauhaus Universität
Marienstrasse 15, D-99423 Weimar, Germany

Tim Rauert, Rheinisch-Westfälische Technische Hochschule

Benno Hoffmeister, Rheinisch-Westfälische Technische Hochschule
Mies-van-der-Rohe-Strasse 1, D-52074 Aachen, Germany

ABSTRACT

In the context of the project DETAILS (Design for optimal life cycle costs of high-speed railway bridges by enhanced monitoring systems), sponsored by the European Research Fund for Coal and Steel, the Erfttal-Bridge near Aachen in Germany was subject of an experimental and analytical investigation into its dynamic characteristics. Relying on the results of this base-line test a two years monitoring system was to subsequently be set up. As a first step of this investigation, an ambient modal test was performed on the Erfttal-Bridge. Applying the EFDD system identification method, 13 modes with a natural frequency between f = 3.7 Hz and f = 41.1 Hz could be identified. Updating of a finite element model using a genetic optimization algorithm yielded MAC values between 1.00 and 0.81 for modes No. 1 to No. 7. Considering the large number of uncertainties within the model, this result is acceptable. The main unknowns are the behavior and influence of the ballast. The ballast is distributed continuously over the two structurally separated bridge girders and across the gaps at the abutments. Further uncertainties are the effect of the rails being continuous over the bridge and the adjacent track sections as well as the stiffness of the elastomeric bearings.

THE BRIDGE

The Erfttal-Bridge consists of two straight, parallel composite filler beam girders, the northern and the southern bridge, separated by a 2 cm gap. There is a 4 m difference in the longitudinal position of the two girders (Fig.1). Each girder is a simple beam with a span length of roughly 25 m (Fig. 2). The two 1.1 m deep and 5.3 m wide girders are steel/concrete composite slabs with eleven 1 m deep rolled steel beams HEM 1000 encased in concrete. The distance between two neighbouring steel beams is about 0.5 m (Fig. 3). Due to an unknown reason, the concrete quality is not the same for the two girders (B25 and B35 respectively). Each girder carries one ballasted railway line. The bridge is used by normal- and high-speed passenger trains as well as by freight trains.

Figure 1 gives further details on the bridges' situation. Adjacent to the northern and the southern Erfttal bridges, the S-Bahn bridge can be seen. This S-Bahn Bridge is an old steel construction used by local railway traffic and is not subject of this paper. The parameters of the highway underneath the railway bridge can also be seen in Figures 1 and 2: Two 4.3 m traffic lanes to the left, the adjacent grass strip and the sidewalk/bikeway to the right.

The measurement point grid as used for the tests on the northern and the southern Erfttal-Bridges is also indicated in Figure 1. This Figure also shows the elastomeric bearing pads' location.

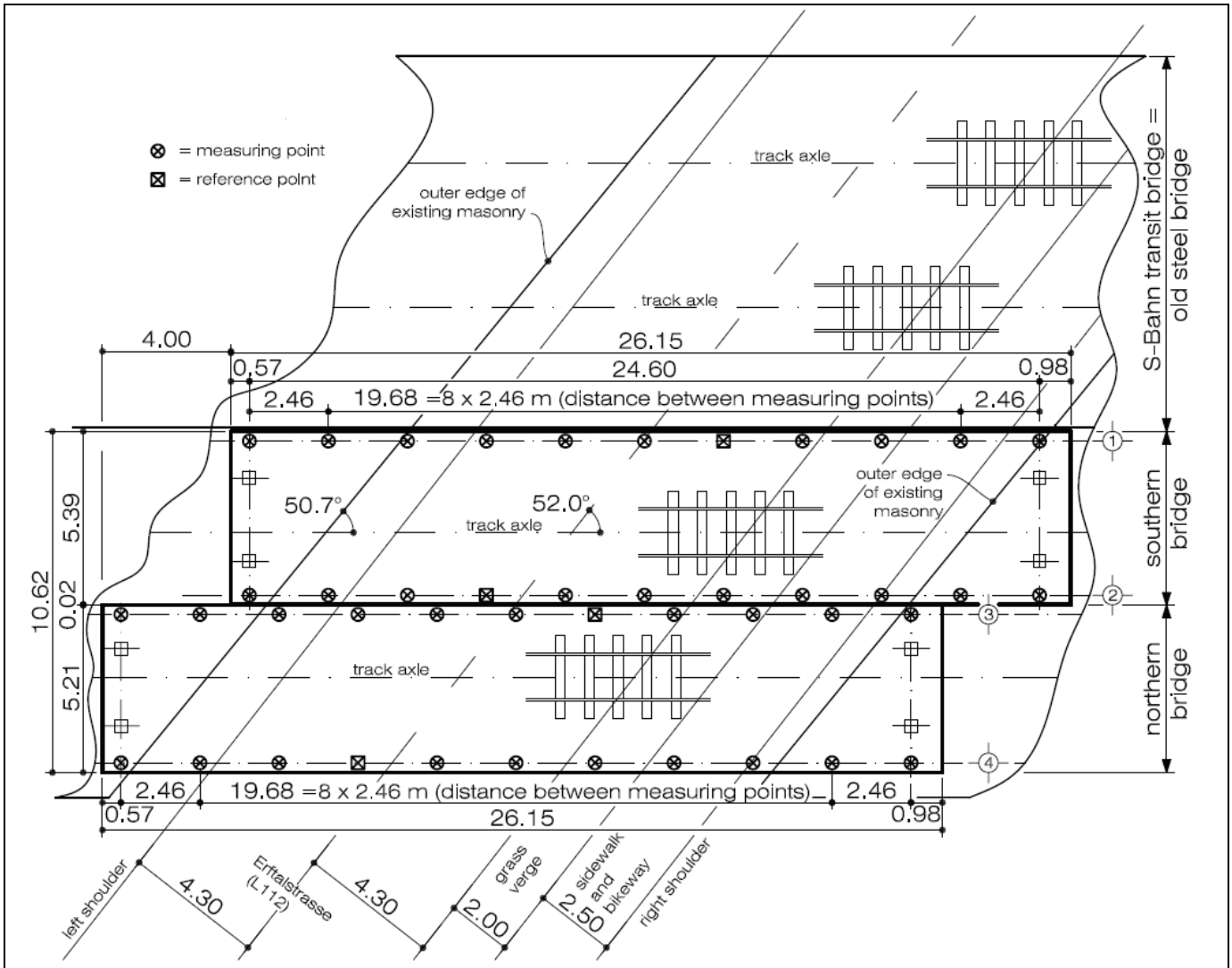

Fig.1: Erfttal-Bridge, plan view. Dimension in meters. The northern and southern bridges are subject of this paper.

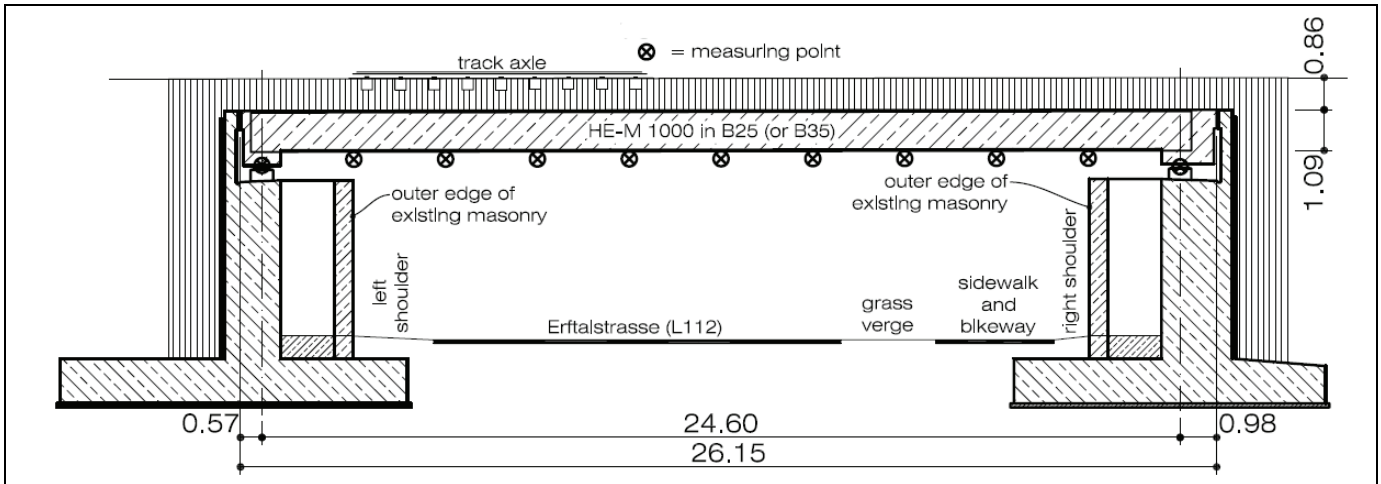

Fig.2 : Erfttal-Bridge, longitudinal section. Dimensions in meters.

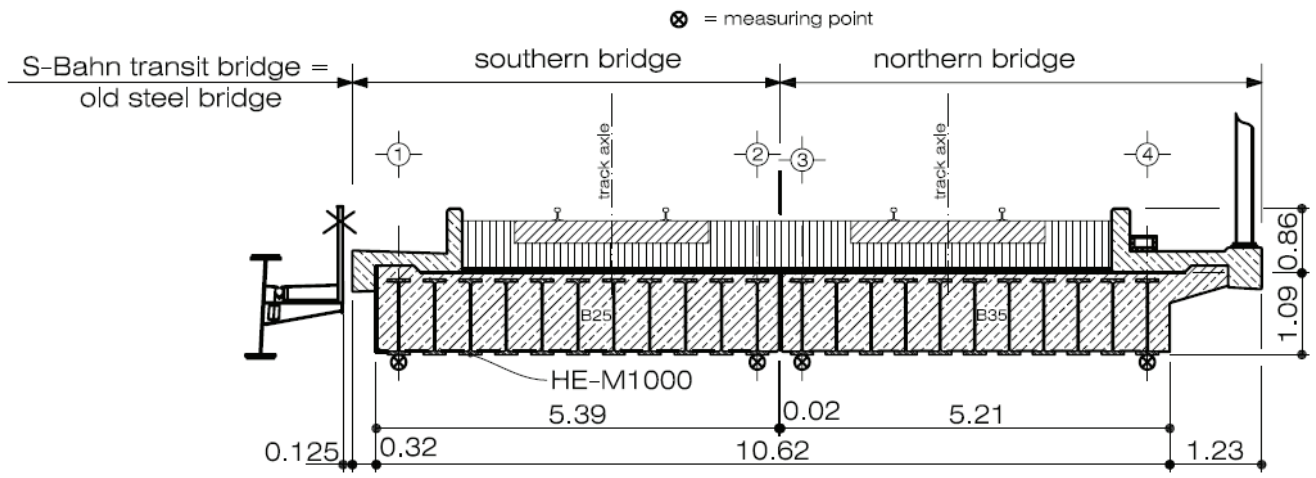

Fig.3: Erfttal-Bridge, cross section. Dimensions in meters. The measurement point lines 1 to 4 correspond to the ones given in Figure 1.

AMBIENT VIBRATION TESTS; INSTRUMENTATION

The important questions to be answered through the tests were: a), what is the behavior of the joint between the two girders, and b), what is the influence of the elastomeric bearing pads? As a consequence, the layout of the instrumentation was quite straightforward. The girders had to be instrumented all along the joint and the girders had also to be instrumented close to the bearings. To being able to distinguish between bending and torsion, each girder was instrumented at the two extreme steel beams. This led to a quite dense grid of 44 measurement points. The number of references was chosen to 4. To cover the 40 remaining points in four setups, 10 roving sensors were necessary. The sensor orientation was always vertical. Two additional channels were used to check the behavior of the bridge in the transverse and longitudinal horizontal directions. This is however not subject of this paper.

As also discussed later, the layout of the references' position and the sequence of the measurement points to be covered by the four setups was heavily influenced through logistic boundary conditions. The result of these discussions and optimizations are presented in Figures 4 to 7. Setups 1 and 2 were performed on day 1, setups 3 and 4 on day 2. The reference points No 7, 15, 29 and 37 had to be accessible on both days.

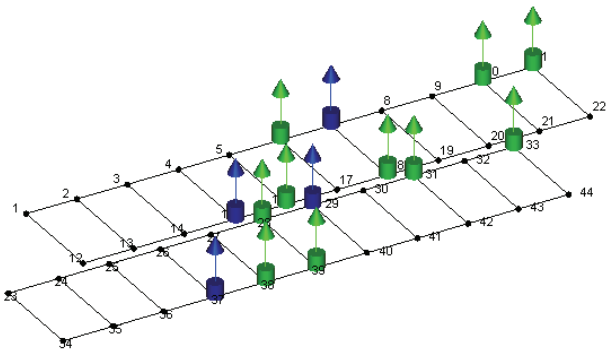

Fig. 4: Instrumentation for setup 1, day 1. Top: Northern bridge, Bottom: Southern Bridge. Blue: reference points, Green: rovers.

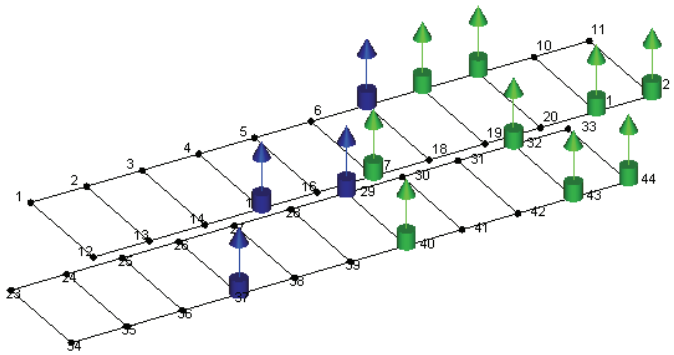

Fig. 5: Instrumentation for setup 2, day 1. Comments see Figure 4.

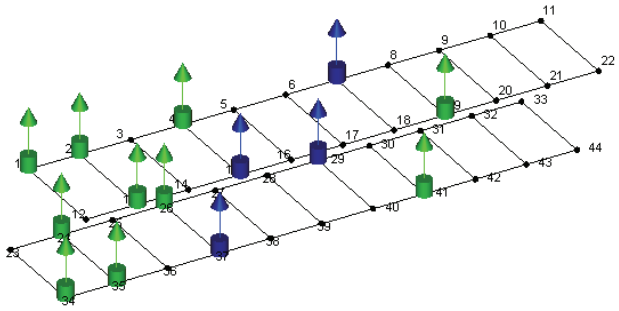

Fig. 6: Instrumentation for setup 3, day 2. Comments see Figure 4.

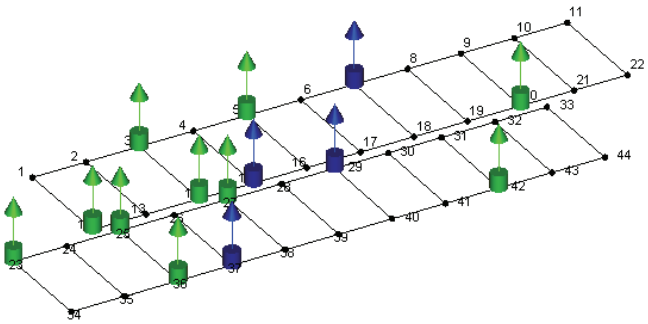

Fig. 7: Instrumentation for setup 4, day 2. Comments see Figure 4.

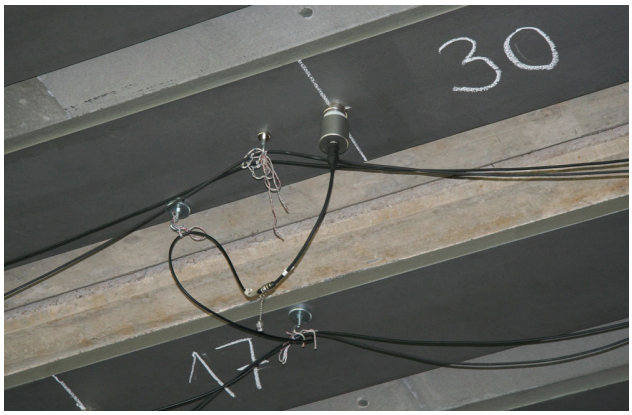

Fig. 8: Close-up of a sensor and of a cable fixation using a magnet.

The sensors used were PCB 393B31 with a sensitivity of 10 V/g (Fig. 8). The sensors were fixed to the steel beams with magnetic supports (Fig. 8). An intermediate plastic layer provided electric isolation of the sensors. With bridges used by electrically driven trains, this is quite essential.

To minimize the headway used by the instrumentation, the cables were fixed to the steel girders with small magnetic devices every two to three meters.

The signals measured were conditioned with an LMS Pimento 16-channel front-end. The sampling rate was chosen to s = 500 Hz, digitization was performed with a 24 bit resolution. These values were chosen to also be able to acquire signals measured during train passages.

AMBIENT VIBRATION TESTING PROCEDURES

Several logistic boundary conditions had to be taken care of. The bridge top side was not accessible. Testing time was limited to two days and 6 hours each (9 am to 3 pm). The reason for this was that the highway traffic underneath the bridge could be reduced from two lanes to a single lane during these time windows only (Figs. 1 and 9). Fortunately, a green strip (being paved underneath the bridge only, Fig. 9) and a pedestrian/bicycle lane were adjacent to one side of the two traffic lanes. This allowed for some air to breathe on one side of the traffic lanes. The measurement van could be placed on the green strip and the strip could also be used to distribute the cables in the transverse bridge direction on the terrain. There was no free room on the other side of these lanes (Figs. 1 and 9).

No critical interference between road traffic and instrumentation occurred during day 1, when the traffic lane adjacent to the measurement van was closed (Fig. 9). On day 2, most of the cables had to cross the lane being now open to traffic (Fig. 10). This was quite challenging because the highway is heavily trafficked with large and high tractor-semitrailers. The headway between the vehicle's roof and the sensors was theoretically something like 0.5 m.

Another challenge was choosing the measurement chain sensitivity and the time windows to store. On the one hand, an ambient test was to be performed. For this purpose, time windows should be available where no train was crossing the bridge. Then, the measurement chain sensitivity should be as high as possible. The train schedule on this bridge is so dense that for each net setup time of roughly 1.5 hours one or two time windows with ambient conditions could be identified from the time table only.

On the other hand, some crossings of high-speed trains should also have been acquired. Here, the measurement chain sensitivity should be such that no overloads would occur while converting the data from analog to digital.

Fig. 9: View underneath the Erfttal Bridge on measurement day 1. From left: Traffic lane open to traffic, closed traffic lane, paved “green strip” where the black measurement van is located”, bicycle/pedestrian lanes.

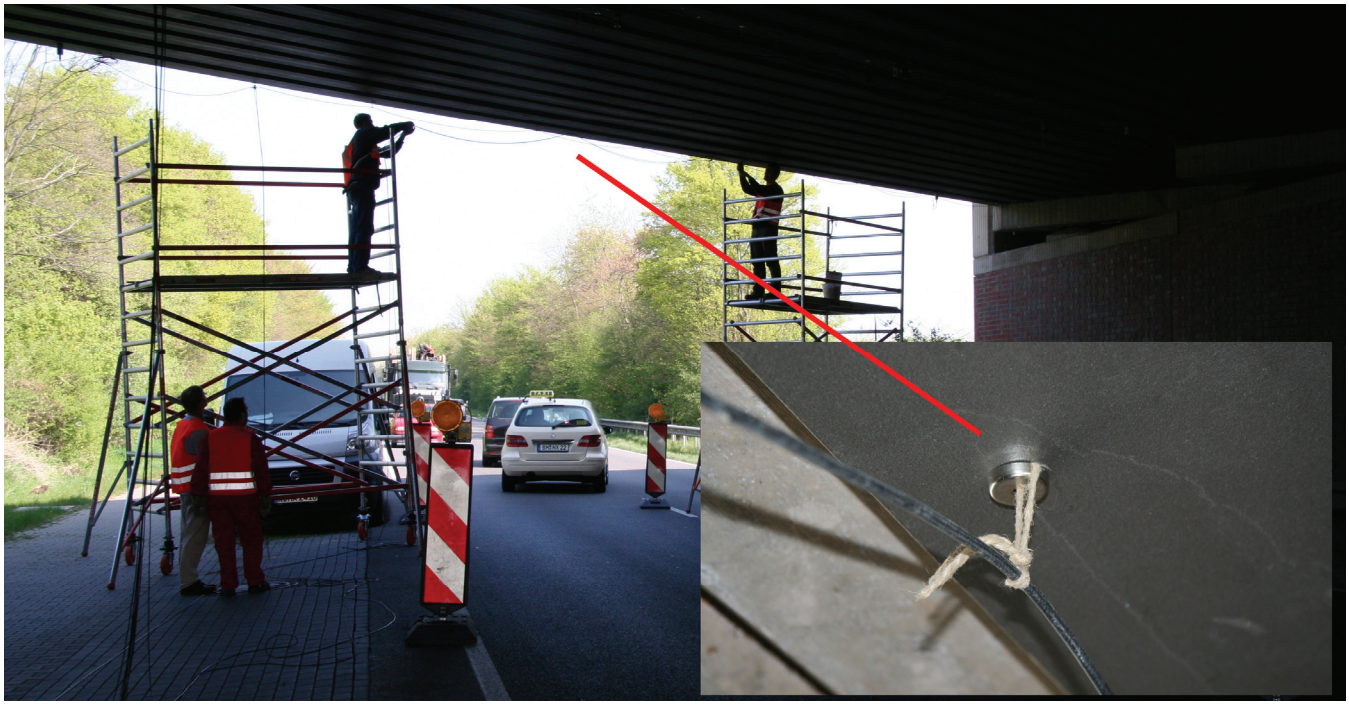

Fig. 10: View underneath the Erfttal Bridge on measurement day 2. View direction reverse to the one in Figure 9.

During the two days of measurement, 23 files were acquired. As the trains did not really keep the theoretical schedule, all files with "ambient" conditions had to be truncated because an unexpected train had appeared, mainly at the end of the time window acquired. For this purpose, a MatLab routine was written which allowed cutting a "good" piece of signal out of a measured signal. The LMS Pimento software does not allow such a signal treatment.

Finally, the dynamic characteristics of the bridge could be extracted from files with ambient conditions for each setup of a minimum T = 410 s length. Some train passages could also be acquired successfully. This will not be discussed here.

AMBIENT VIBRATION TESTS; SIGNAL PROCESSING AND RESULTS

Applying the Artemis Software Suite and making use of the EFDD (Enhanced Frequency Domain Decomposition) routines allowed identification of 13 bridge modes in the frequency range f = 3.68…41.1 Hz. By decimating the data by a factor of 5, the Nyquist frequency was reduced to f = 50 Hz. The SVD diagram presented in Fig. 11 shows that the number of projection channels was chosen to 4. The number of frequency lines for f = 0…50 Hz was chosen to 512.

Application of the Artemis SSI routines yielded an additional mode 4a at f = 13.71 Hz. Whereas mode 4 at f = 13.24 Hz is the second bending mode with the two girders being in phase, mode 4 is the second bending mode with the girders being out of phase. It is not clear why it was not possible to separate these modes using the EFDD technique.

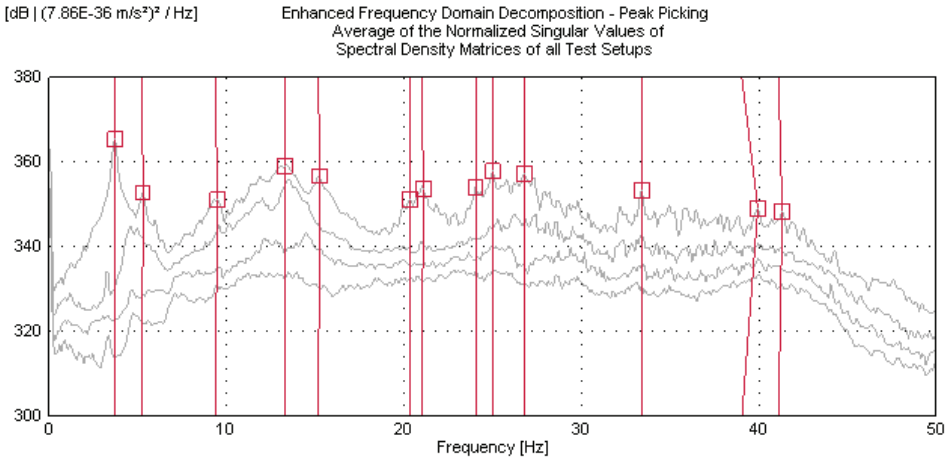

Fig.11: EFDD SVD diagram as determined through application of Artemis Extractor routines.

Mode	Freq. f [Hz]	σf [Hz]	Damp. ς [%]	σς [%]	**Mode**	Freq. f [Hz]	σf [Hz]	Damp. ς [%]	σς [%]
1	3.68	0.01	2.56	0.11	**7**	20.98	0.23	0.65	0.19
2	5.24	0.03	2.76	0.24	**8**	24.05	0.09	0.52	0.20
3	9.36	0.13	2.05	0.69	**9**	24.96	0.23	0.56	0.23
4	13.24	0.13	0.87	0.64	**10**	26.81	0.03	0.86	0.94
4a	13.71	0.17	2.96	0.89	**11**	33.4	0.01	0.24	0.02
5	15.18	0.06	1.22	0.20	**12**	39.04	1.52	0.28	0.15
6	20.36	0.10	0.47	0.28	**13**	41.11	0.15	0.20	0.08

Fig. 12: Natural frequency f, standard deviation σf, Damping in percent of critical, ς, and standard deviation, σς,for the 14 modes identified for the Erfttal Bridge.

FINITE ELEMENT MODELLING

Here, the first step of the finite element modelling procedure of the bridge is presented (Fig. 13). The concrete of the slab is modelled by 4-node shell elements and the embedded steel I-Sections with 2-node beam elements. Also, the cross beams at the abutments are 2-node beam elements being connected to the slab through constraint equations. According to [1], the elastomeric bearings are represented through a spring with six degrees of freedom. The mass and stiffness of the ballast is added to the concrete slab. Springs are used to consider the continuous distribution of the ballast across the gap between the two slabs and across the abutments at each end of the bridge. The rails and sleepers are 2-node beam elements, which are connected through springs to each other to model the pads. The rail-sleeper-system is furthermore connected through springs to the slab. The rail is extended 2 m at each end of the bridge to consider the continuous effect of the rail. This part of the rail is connected to the ground by springs. Mass and stiffness of the noise protection wall, the handrail and the edge beam are not considered.

The initial material parameters for steel and concrete are given in [2], the shear modulus of the elastomeric material is given in [1]. The mass of the ballast is set to 2,000 kg/m^3. The main unknown is the stiffness contribution of the ballast in each direction at every point.

To simplify the model concerning the number of design variables for the subsequent model updating it is assumed that the same stiffness is present at each elastomeric bearing and that the concrete and the ballast are homogeneous. Furthermore, presumably no significant damage has occurred to the bridge.

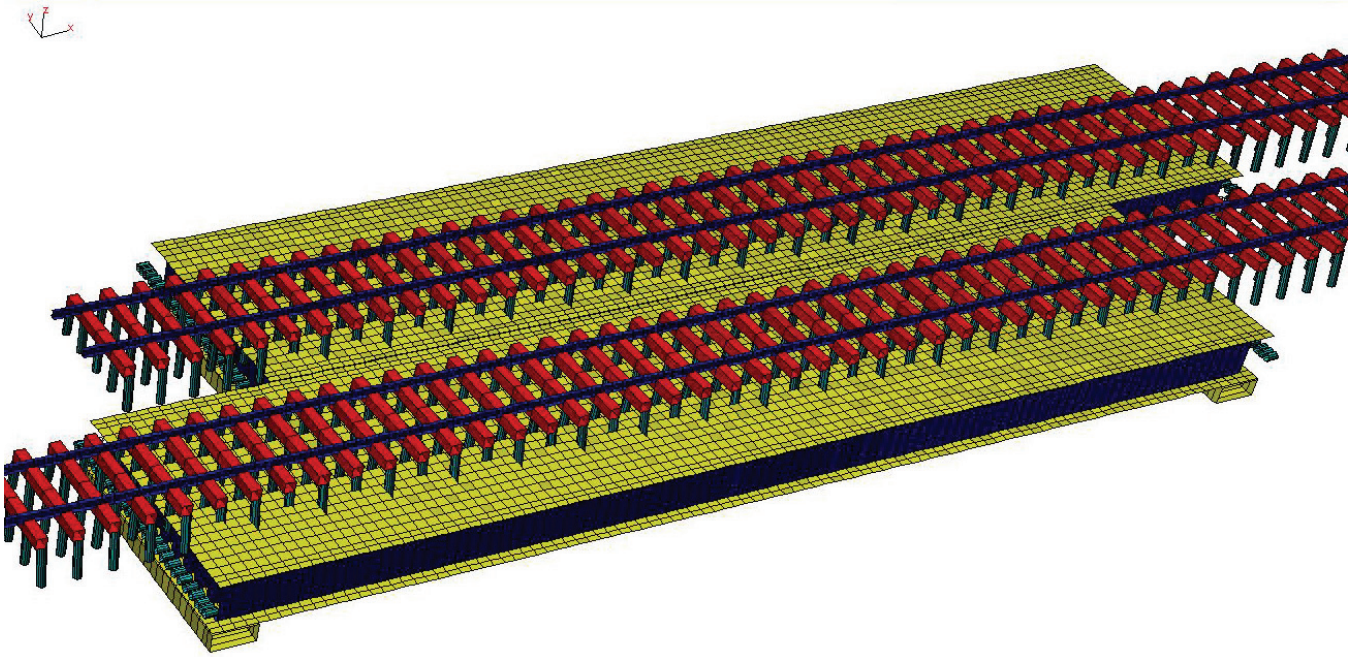

Fig. 13: Finite element model of the Erfttal-Bridge.

MODEL UPDATING

To update the model parameters with respect to the first 7 experimentally identified eigenfrequencies f_i^e and corresponding eigenvectors Φ_i^e of the system a genetic optimisation strategy implemented in [3] is used. The objective function is given by

$z = \sum_{i=1}^{7}\left[\frac{\left\|f_i^e - f_i^n\right\|}{f_i^e}\right] + \sum_{i=1}^{7}\left[1 - MAC(\Phi_i^e, \Phi_i^n)\right]$, where MAC(x,x) is the modal assurance criterion.

The 16 design variables are the Young's moduli and densities of the two concrete types, the shear modulus of the elastomeric material and a set of spring parameters. The eigenfrequencies f_i^n and the eigenvectors Φ_i^n of the updated numerical model are presented in Figs. 14a and 14b. The MAC-values are close to 1.0. Only for modes 5 and 6, which show some irregularities in the identified shapes, MAC-values of 0.81 and 0.82, respectively, have been obtained. However, these results are considered to be sufficient in this case. The updated frequencies are not as good as the mode shapes. Errors of up to 12.85% were obtained.

Mode No.	Freq. f_i^n [Hz]	Error [%]	MAC [-]	Mode Shapes (red: experimentally obtained; blue: result of FE model updating)
1	3.38	-8.15	1.00	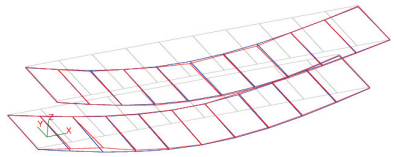
2	5.05	-3.63	0.96	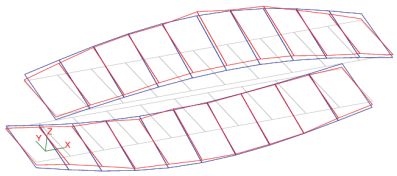
3	10.16	8.55	0.91	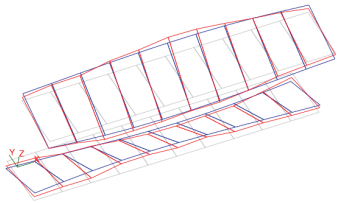
4	11.83	-10.65	0.95	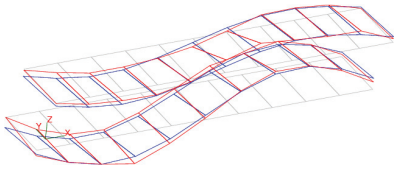
4a	12.93	-5.69	0.94	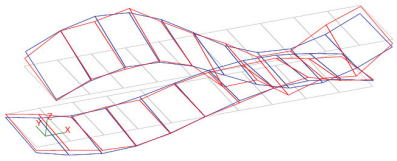
5	13.23	-12.85	0.81	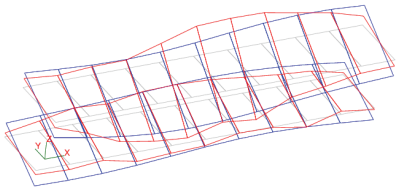

Fig. 14a: Eigenfrequencies and mode shapes of the updated model compared with the results obtained by EFDD/SSI.

Mode No.	Freq. f_i^n [Hz]	Error [%]	MAC [-]	Mode Shapes (red: experimentally obtained; blue: result of FE model updating)
6	20.48	0.59	0.82	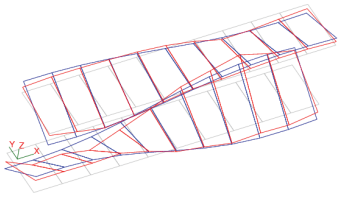

Fig. 14b: Eigenfrequencies and mode shapes of the updated model compared with the results obtained by EFDD.

It is obvious that the finite element model and/or the system identification include some deficits. Furthermore, nonlinear effects may have a significant influence on the system even in the ambient vibration tests. To investigate this issue in detail, a next step will be using a refined finite element model for model updating. Especially, the mass of the noise protection wall may have a considerable influence.

CONCLUSIONS

Both the identification of the modal behaviour and parameters of a finite element model of a typical short span railway bridge are presented in this study. It has been shown that several modes could be identified from relatively weak ambient vibration signals by applying appropriate algorithms.

The combination of both experimental and numerical analyses has been proven to be a successful methodology for handling identification problems of the kind as described in this paper. Even though the mechanical behaviour of an orthotropic railway bridge with continuous rails on ballast is quite difficult to describe numerically, comparatively good results in model updating have been obtained by applying a genetic optimisation scheme. However, it is expected that further refinements of the initial model will lead to a better agreement of the model's modal parameters with those identified from the tests. Therefore one of the next steps is refinement of the finite element model. The standard deviations of the identified natural frequencies and the accuracy of the extracted mode shapes should be considered in the objective function as well.

ACKNOWLEDGEMENTS

It is gratefully acknowledged that the presented study is part of the European research project DETAILS which is supported by the European Research Fund for Coal and Steel.

REFERENCES

[1] DIN Deutsches Institut für Normung e.V.: DIN EN 1337-3: Lager im Bauwesen – Teil 3:Elastomerlager; Deutsche Fassung EN 1337:2005

[2] Schneider, Klaus-Jürgen: Bautabellen für Ingenieure. 13. Auflage, Werner Verlag, 1998.

[3] optiSLang –the optimizing Structural Language. Version 2.1, Weimar, Dynardo GmbH, www.dynardo.de